

Ductile Fracture of Aluminum

G. Y. Chin, W. F. Hosford, Jr., and W. A. Backofen

The ductile fracturing process was studied in single-crystal and polycrystalline aluminum deformed in tension over a temperature range from 295° to 4.2°K. At temperatures as low as 77°K, the fracture of "inclusion-free" material, including zone-refined aluminum, was by rupture (~100 pct RA). At 4.2°K, fracture was brought on by adiabatic shear. Metallographic examination did not disclose any voids or slip-band microcracks, thus negating for inherently ductile metals any mechanism of void nucleation by vacancy condensation or of cracking due to dislocation pile-ups. In high-purity aluminum not treated to be inclusion-free, fracture at temperatures as low as 45°K was of the double-cup type and a result of void formation. The reduction-of-area decreased as temperature was lowered, corresponding to the earlier appearance of voids. Such behavior was rationalized in terms of a larger increase, with decreasing temperature, in the flow stress relative to the strength of the inclusion-matrix interface. Evidence for low-temperature adiabatic shear was found in discontinuous flow at 4.2°K, in the transition to a localized shear fracture at low temperatures, and in the suppression of shear fracture with an elastically hard pulling device. A simple analysis for the initiation of adiabatic shear permitted a general correlation of the various contributing factors. It has been pointed out that the duration of shear depends upon effective mass and elastic stiffness of the deformation system.

IT has long been recognized that fracture* may

*Throughout this paper, the term "fracture" is taken to mean any process that results in the separation of a material into two (or more) parts. Thus rupture as it may be encountered in a tension test leading to 100 pct reduction-of-area is included in this category.

occur in a ductile mode, and that the process can be of great practical as well as general interest. Much information about ductile fracture has also been accumulated over this period, but only recently has an understanding of mechanism begun to appear.

G. Y. CHIN is with Bell Telephone Laboratories, Murray Hill, N.J. W. F. HOSFORD, JR., Member AIME, formerly with Massachusetts Institute of Technology, is now Associate Professor, Department of Chemical and Metallurgical Engineering, University of Michigan, Ann Arbor, Mich. W. A. BACKOFEN, Member AIME, is professor, Department of Metallurgy, Metals Processing Laboratory, Massachusetts Institute of Technology, Cambridge, Mass. This paper is based on a thesis by G. Y. CHIN submitted to the Massachusetts Institute of Technology in partial fulfillment of the requirements for the degree of Doctor of Science.

Manuscript submitted April 29, 1963. IMD

Ludwik,¹ in 1926, first reported fracture in a tensile specimen starting with a central crack in the necked section. Since then, other studies have disclosed that such cracks may form by the coalescence of voids nucleated in this region where hydrostatic tension is highest.²⁻⁴ Rogers⁴ and Crussard *et al.*⁵ have emphasized void formation and reorientation along localized shear bands as a mode of crack propagation. Pines⁶ has considered the tensile rod as a bundle of fibers joined by weak interfaces, which subsequently separate to allow individual fiber contraction. The notion of cavity growth and coalescence by purely plastic processes was discussed by Cottrell,⁷ who added that the tensile reduction-of-area ought not to be sensitive to temperature. On the other hand, it has been observed that the reduction-of-area is greatly increased if tests are carried out at high temperatures⁸ or under high hydrostatic pressure.⁹

Fracturing anisotropy in wrought products lends support to the idea of void formation from pre-existing flaws strongly aligned by earlier processing.¹⁰⁻¹² There is evidence that many voids result from the fracturing of inclusions or separation at the inclusion-matrix interface.^{2,3,5} Another possibility is that voids grow out of pore volume produced in the initial solidification and never fully removed in later working. In general, a structure of particles, pores, and weak interfaces can be expected, at least in materials of engineering interest.

Vacancy condensation has been suggested as an alternative mechanism of void formation for materials considered to be inclusion-free.¹³ Yet experience has shown that tensile reduction-of-area increases with purity, to the extreme of rupture as so often observed in single crystals.

Adiabatic shear has an important bearing on ductile fracture. It occurs when the decrease of flow stress, as a result of local temperature rise from heat generated during straining, becomes larger than the increase due to strain and strain-rate hardening. As demonstrated by experiments on punching of plates,¹⁴ a large temperature rise may be brought about by rapid straining. Adiabatic flow as a result of the high strain rate reached in an ordinary tensile specimen just prior to separation may account for the cone formation in cup-and-cone fracture;¹⁴ evidence of such local heating has been presented.¹⁵ For geometrical reasons, however, pure sliding along the conical surfaces is unlikely, and separation under tensile forces is probably an important accompanying feature of the shear.⁷ In deformation processing operations, a high shear-strain rate may exist at boundaries between plas-

tic and elastic fields; resultant local temperature rise could lead again to adiabatic shear. At very low temperatures, the specific heat is much reduced. Hence a large temperature rise can occur even during quasi-static tension, the subsequent adiabatic shear being responsible for discontinuous slip and shear fracture.¹⁶ It has been further suggested that the amount of unstable flow associated with adiabatic shear must be influenced by the elastic energy stored in the deforming system.¹⁴ In confirmation, it has been shown that the conical shear surface in an Armco iron tension specimen is suppressed with an elastically stiffened testing device.¹⁷

The role of dislocations in ductile fracture, beyond that in accomplishing slip, is not yet clear. Dislocation pile-up cracking is known to be important when fracture involves cleavage. However, its contribution in inherently ductile metals such as copper and aluminum is in question at present, for one reason because there is no clear evidence of dislocation pile-ups in these materials, even after heavy straining.¹⁸ Beavers and Honeycombe,¹⁹ on the other hand, have interpreted their findings on copper and aluminum in terms of the pile-up mechanism.

Still less clear is the nature of "hair-line" cracking as reported by Ludwik,¹ Puttick,³ and Neimark.²⁰ Although no study has been made of this phenomenon, the possibility of an association with subgrain boundaries cannot be overlooked. Subboundary cracking has been observed in fatigue testing²¹⁻²³ as well as in explosive deformation,²⁴ while substructure formation during heavy straining has been well-documented.¹⁸

The background in ductile fracture thus involves a complex interplay among several issues each of which requires clarification before the basic process is completely understood. By combining a number of the important variables in a single test program, it was hoped that the present experiments would contribute to such an end. The work has been based on aluminum in both single-crystal and polycrystalline form, tested in tension over a range of temperatures in "hard" and "soft" machines.

EXPERIMENTAL PROCEDURES

Materials and Specimen Preparation. *Single Crystals.* Starting material was 99.995 wt pct pure Al. Growth was by directional solidification under a helium atmosphere in a horizontal furnace at a rate of 0.4 in per hr. Crystals of [111], [100], and [110] axial orientations were seeded; others were grown

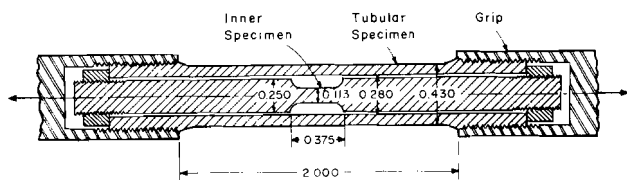


Fig. 1—Sectional view of extra-hard arrangement. Dimensions in inches.

randomly. All were annealed at 600°C for 18 hr and furnace-cooled over a 12-hr period. Orientation was determined by the Laue back-reflection method.

The as-grown crystals had a cross section of 1/4 by 3/16 in. A gage section of about 3/16 by 1/8 in. by 3 in. was produced by masking the ends with Duco cement and then chemically etching in an aqueous solution of 5 pct NaOH and 10 pct NaNO₂.²⁵ Prior to testing, most samples were electropolished in a solution of 5 parts methanol and 1 part perchloric acid cooled to below -30°C. Seating alignment during testing was assured by casting Wood's metal into split-collar steel grips containing the enlarged ends of the sample.²⁵

Polycrystals. Polycrystalline specimens were machined into rods of 0.112-in. diam with 1.125-in. gage length. Three kinds of material were tested.

1) **Wrought.** Samples were prepared from the 1/4-in.-diam as-received stock of 99.993 wt pct pure Al. The original grain diameter, approximately 0.025 mm, was retained upon annealing at 300°C for 2 hr. Several samples were annealed at 500°, 450°, and 400°C to produce grain sizes of 0.7, 0.35, and 0.15 mm diam, respectively. Metallographic examination revealed some fine strings of inclusions parallel to the specimen axis. The density of inclusions was somewhat higher at the center.

2) **"Purified"**. To minimize the number of inclusions, a length of 99.995 wt pct Al single crystal was grown by the usual directional solidification and,

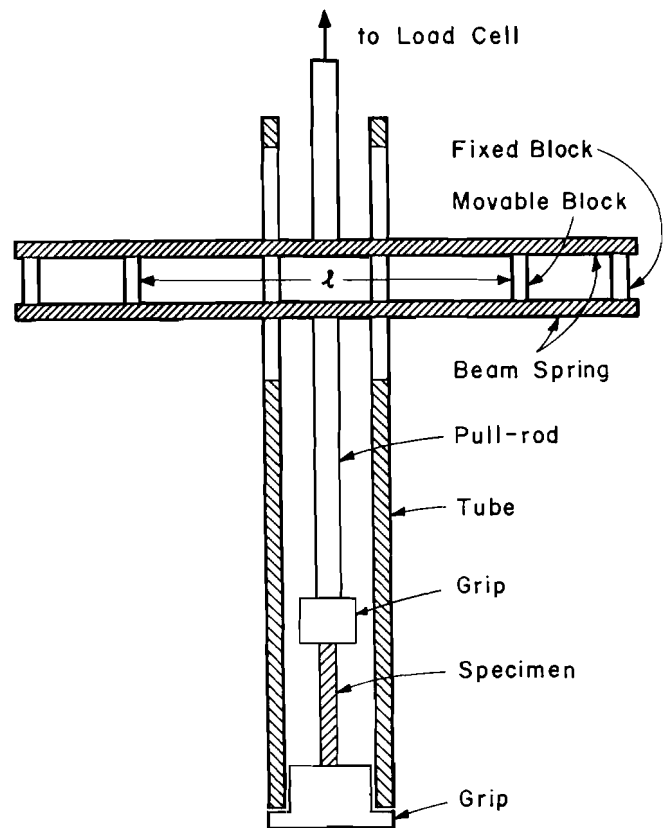


Fig. 2—Soft-machine arrangement. *l* is effective length of spring.

after discarding the impure end, was converted to polycrystalline material with a grain size of about 0.1 mm diam by swaging and recrystallization. Examination of this material revealed hardly any inclusions.

3) **Zone-refined.** To assure "complete" freedom from inclusions, specimens were made from previously zone-refined aluminum with each impurity level believed to be below 0.1 ppm. This material recrystallized at room temperature after swaging. The grain size, though not uniform, averaged about 0.3 mm diam.

Testing. The samples were tested mostly in a hard-type machine described elsewhere.^{16,25} Basically, a screw-driven load cell was coupled to a pull-rod, which moved within a tube that was mounted rigidly in a vertical position. The lower end of the rod was attached to the upper grip on the specimen. The bottom grip on the specimen was secured, in turn, to the lower end of the tube. This "standard hard machine" had a spring constant of about 25,000 lb per in.

The effect of stored elastic energy on adiabatic flow and shear fracture at 4.2°K was also studied with an extra-hard arrangement achieved by using a short specimen of small cross section surrounded by a longer tubular specimen of larger cross section, Fig. 1. Thus any sudden elongation in the inner specimen would be restrained by the less highly stressed outer specimen.

The testing machine was made elastically much softer by inserting a series of beam springs between the load cell and the pull-rod, Fig. 2. The spring constant of the soft arrangement could be lowered to about 300 lb per in. by changing the effective length of the springs; the value of 300 lb per in. applies to all of the soft-machine tests reported below.

Experiments were made at 295°K (room temperature), 77°K (immersion in liquid nitrogen), and

Table I. Summary of Flow and Fracture Data Obtained with the Standard Hard Machine of Spring Constant 25,000 Lb Per In.

Test Temperature, °K	295	77	45	40	30	4.2
	Type of Fracture*					
Single crystals	R	R	—	—	—	S
	Polycrystals					
Wrought material, 0.025 mm	DC	DC	DC	S	S	S
"Purified" material, 0.1 mm	R	R	—	—	—	S
Zone-refined, 0.3 mm	R	R	—	—	—	S
	Type of Load Record**					
Single crystals	a	a	—	—	—	c, d
	Polycrystals					
Wrought material, 0.025 mm	a	a	b	b	b	b
"Purified" material, 0.1 mm	a	a	—	—	—	c, d
Zone-refined, 0.3 mm	a	a	—	—	—	b, c
	Percent Necking-at-Fracture, † Pct N					
Single crystals	100	100	—	—	—	0 → 20
	Polycrystals					
Wrought material, 0.025 mm	99	97	87	72	68	65
"Purified" material, 0.1 mm	100	100	—	—	—	0 → 30
Zone-refined, 0.3 mm	100	100	—	—	—	30 → 70

*DC—double-cup; S—shear; R—rupture.

**"Type of Load Record" refers to curves in Fig. 4.

† Pct N = 100 (1 - A_f/A_n) where A_f and A_n are the cross-sectional areas at fracture and at start of necking, respectively.

Dash (—) indicates no test.

4.2°K (immersion in liquid helium), with particular emphasis on 4.2°K because of the interest in adia-

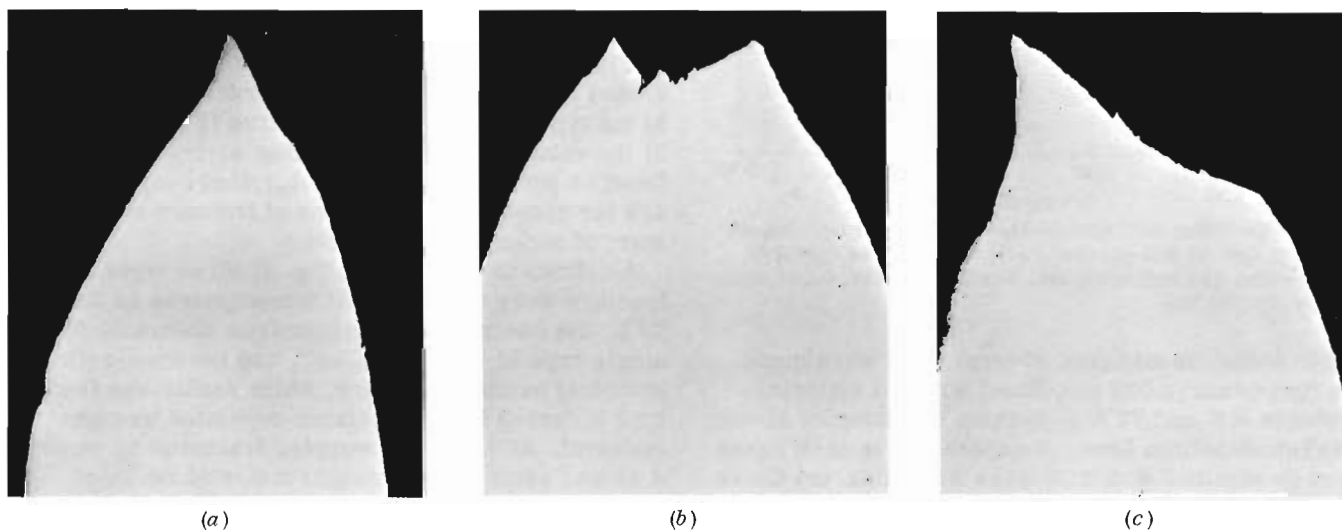


Fig. 3—Types of fracture in aluminum: (a) rupture (single crystal tested at 295°K); (b) double-cup (fine-grained wrought sample tested at 45°K); and (c) shear (fine-grained wrought sample tested at 4.2°K). The specimens were sectioned along a plane containing the loading axis so as to illustrate the type of fracture. About X40. Reduced approximately 21 pct for reproduction.

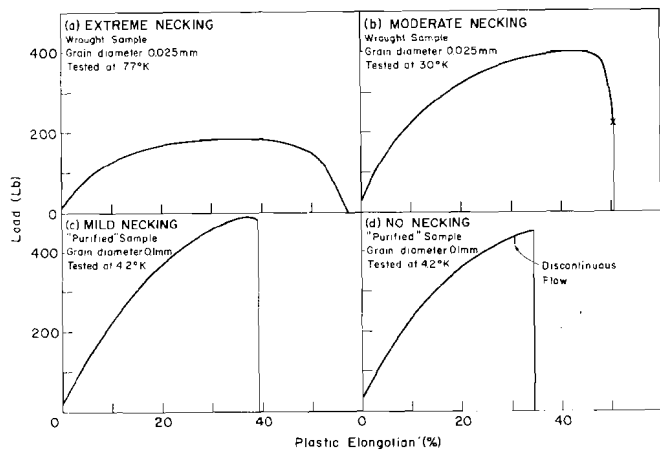


Fig. 4—Types of load record obtained with the standard hard machine.

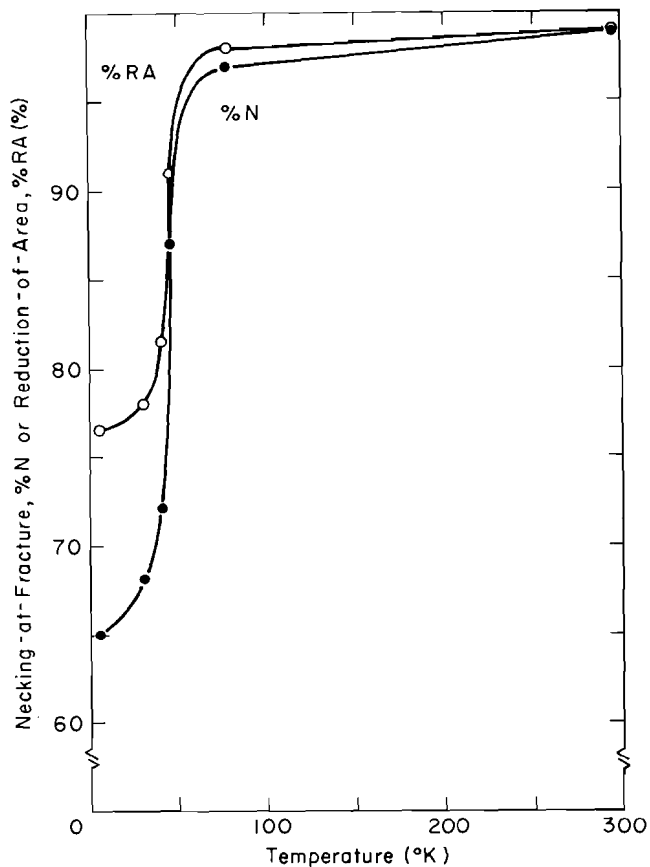


Fig. 5—Variation with temperature of percent necking-at-fracture (pct N) and percent reduction-of-area (pct RA) for the fine-grained material. Grain diameter, 0.025 mm; purity, 99.993 pct.

batic shear. In addition, several tests were made on fine-grain (0.025 mm diam) wrought material between 4.2° and 77°K by raising the samples above the liquid-helium level. Temperature in such cases was determined with a 30-gage Au-2.1 at. pct Co vs Cu thermocouple attached in the vicinity of the specimen, using the liquid helium as the cold junction. This method was somewhat crude, the absolute uncertainty probably being about $\pm 4^\circ\text{K}$ with an uncertainty between tests of about $\pm 2^\circ\text{K}$.

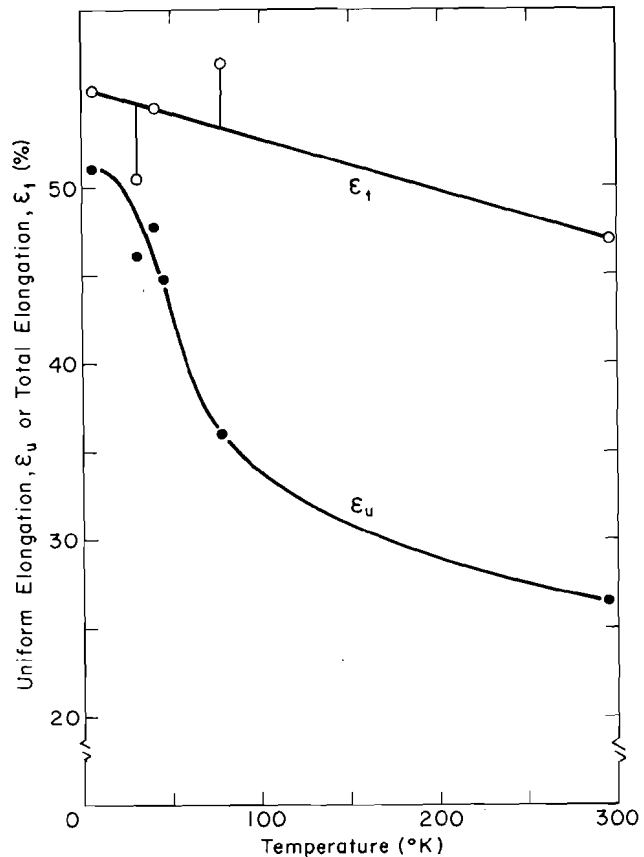


Fig. 6—Variation with temperature of uniform elongation and of total elongation for the fine-grained wrought material. Grain diameter, 0.025 mm; purity, 99.993 pct.

Load was recorded as the output of a wire-resistance strain-gage bridge. Extension was measured by recording cross-head motion. The over-all strain rate was about $3 \times 10^{-4} \text{ sec}^{-1}$.

RESULTS

General Behavior Patterns. The results of tensile testing at various temperatures with the standard hard machine are summarized in Table I and in Figs. 3 through 7. Three sets of data are presented in Table I: 1) the type of fracture (Fig. 3), 2) the type of load-elongation curve (Fig. 4), and 3) the values of percent "necking-at-fracture", defined as $\text{pct } N = 100(1 - A_f/A_n)$ where A_f and A_n are the cross-sectional areas at fracture and at the start of necking, respectively.

As shown in Table I and Fig. 3, three types of fracture were observed. At temperatures as low as 77°K, the essentially inclusion-free materials (the single crystal, the "purified", and the zone-refined samples) exhibited *rupture*, while *double-cup* fracture occurred in the inclusion-populated wrought material. At 4.2°K, all samples fractured by *shear*. A closer study of the wrought material revealed that a transition from double-cup to shear took place between 40° and 45°K.

The type of load-elongation curve, as designated in Fig. 4, indicates the severity of necking. A more definitive quantity, however, is the percent necking-

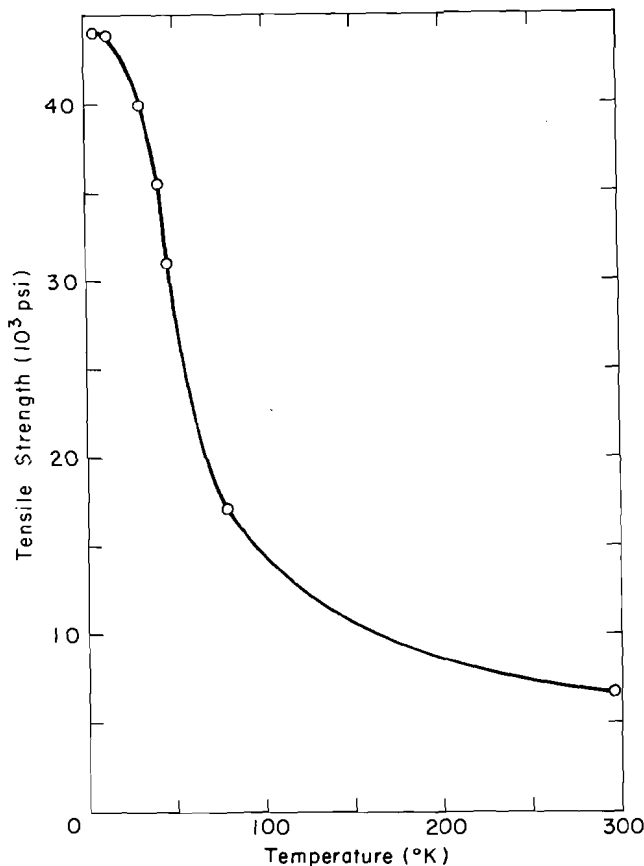


Fig. 7—Temperature dependence of the tensile strength of the fine-grained wrought material. Grain diameter, 0.025 mm; purity, 99.993 pct.

at-fracture (pct N). Thus pct N has a value of 100 for rupture and is zero when necking is absent, the latter value characterizing some single crystals and "purified" polycrystals tested at 4.2°K, Table I. Contrary to Cottrell's suggestion,⁷ necking-at-fracture decreased with lower temperature; values for the fine-grained wrought material, taken from Table I, are presented in Fig. 5, together with data on the percent reduction-of-area. The difference between the two curves at very low temperatures is the result of an increase with falling temperature in the uniform elongation, plotted in Fig. 6 from observations on load maxima; such a trend is related to the generally higher and more persistent rate of strain hardening at the lower temperatures. The total elongation in Fig. 6 was relatively insensitive to temperature since the elongation after necking was larger at higher temperatures. The variation of tensile strength with temperature is shown in Fig. 7 for the fine-grained wrought material; a steep rise at temperatures below 77°K is noted. Values of both uniform elongation and tensile strength compare favorably with the data of Carreker and Hibbard.²⁸

Grain-Size Dependence of Fracture Stress at 4.2°K. Values of true tensile fracture stress, defined as $\sigma_f = P_f/A_f$ where P_f and A_f are, respectively, the load and cross-sectional area at frac-

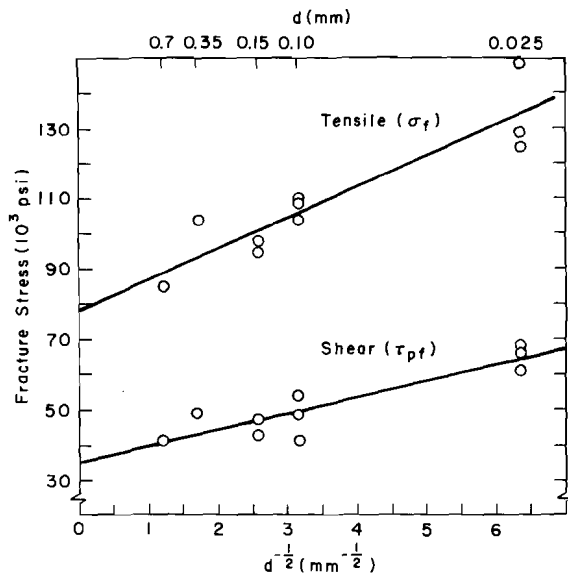


Fig. 8—Fracture stress vs grain size for wrought material tested at 4.2°K. The 0.1-mm-diam data were taken from the "purified" material. Straight lines were drawn using the method of least squares.

Table II. Values of the True Tensile Fracture Stress and of the Resolved Shear Stress at Fracture in Single Crystals Tested at 4.2°K. Initial Axial Orientations are shown in Fig. 10.

Specimen	$\sigma_f, 10^3$ Psi	$\tau_{sf}, 10^3$ Psi
S1	62.2	23.0
S2'	50.6	20.4
S3	56.9	21.8
S3'	56.4	21.9
S4	73.6	20.1
S5	79.0	21.5
S6'	45.8	20.6
S6	42.2	19.1
S7	79.3	21.6
S7'	83.8	22.8
S8	56.9	23.2
S9	54.8	22.2
S10	57.7	23.6
S10'	50.6	20.7
S11'	49.0	*
S12	51.0	22.9
S12'	53.1	24.2
S13	44.2	19.6
S15	45.2	19.9
S16	79.8	21.7
[111]**	77	21.0
[100]**	57.5	23.5

*Laue spots at fracture were diffuse and final orientation could not be determined.

**From Ref. 25.

ture, are listed in Table II for the single crystals tested at 4.2°K. Also presented in Table II are the values of resolved shear stress at fracture, defined as $\tau_{sf} = m_f \sigma_f$ where m_f is the Schmid orientation factor for resolving the shear stress on the most highly stressed slip system at fracture. The value of m_f was determined from the Laue back-reflection photograph obtained near the fracture region. Single crystals fractured at this temperature of 4.2°K

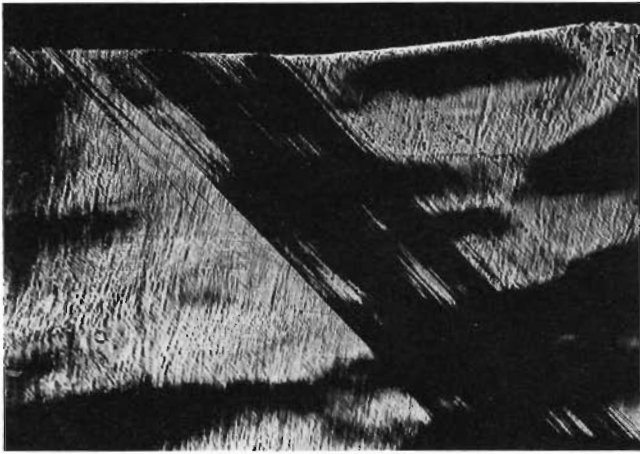


Fig. 9—Slip cluster associated with discontinuous flow. Crystal S2' deformed in tension at 4.2°K; orientation in Fig. 10. X100. Reduced approximately 25 pct for reproduction.

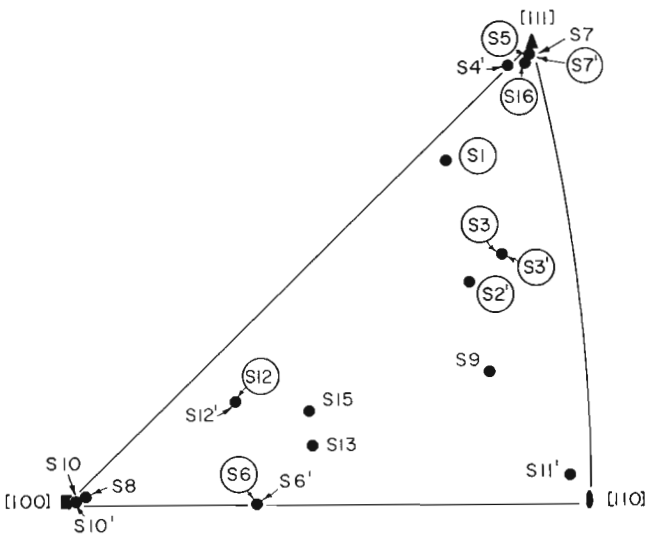


Fig. 10—Initial axial orientations of single crystals tested at 4.2°K. Encircled specimens exhibited discontinuous flow.

by localized shear along slip planes (see Fig. 11) after little or no necking (Table I). Therefore, both σ_f and τ_{sf} are considered to be meaningful. It is noted that, while σ_f varied from about 42,000 to 80,000 psi, τ_{sf} was remarkably constant at an average level of approximately 22,000 psi. Constancy of resolved shear stress at fracture for Al-5.5 wt pct Cu single crystals tested from 77° to 373°K has been reported by Beevers and Honeycombe.²⁷

For the polycrystals tested at 4.2°K, the shear-fracture plane was oriented at an angle, α , of 45 to 65 deg from the tensile axis. Values of both true tensile stress σ_f and shear stress at fracture (the latter defined as $\tau_{pf} = \sigma_f \cos \alpha \sin \alpha$) were proportional to the inverse square root of grain diameter, d (Fig. 8). Recently, Armstrong *et al.*²⁸ and Armstrong²⁹ have pointed out that propagation of plastic flow in a polycrystal requires internal stress concentrations proportional to $d^{-1/2}$. They predicted that the value of tensile flow stress, σ_0 , from ex-

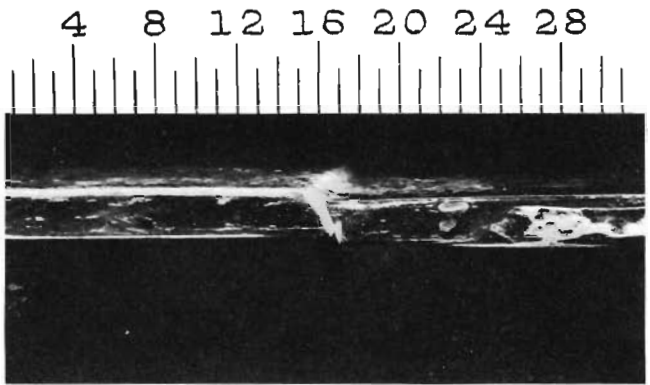


Fig. 11—Localized shear along active octahedral slip planes preceding shear separation. Crystal S3' (see Fig. 10) tested in tension at 4.2°K; dimensions indicated are multiples of 1/32 in.

trapolation to $d^{-1/2} = 0$ would correspond to the average flow stress of a single grain in the aggregate: that is, the flow stress of a polycrystal as analyzed by Taylor.³⁰ On this basis, $\sigma_0 = m\tau_s$ and $\tau_0 = (m/2)\tau_s$ (since $\sigma_0 = 2\tau_0$), where m is the Taylor factor of 3.1 and τ_s is the single-crystal shear strength. In the present case of shear fracture at 4.2°K, $\tau_{sf} = 22,000$ psi for single crystals, Table II. Accordingly, the calculation gives $\sigma_0 = 68,200$ psi and $\tau_0 = 34,100$ psi, whereas the extrapolated values from Fig. 8 are 78,000 and 35,300 psi, respectively. This favorable correlation between σ_0 and τ_0 from Fig. 8 and the experimental τ_{sf} strongly indicates that low-temperature shear fracture in both single crystals and polycrystals proceeds by crystallographic shear rather than by dislocation pile-up cracking.

Low-Temperature Adiabatic Shear. Evidence for low-temperature adiabatic shear was found in the appearance of discontinuous flow at 4.2°K, in the transition from one type of fracture to another at low temperatures, and in the results of machine-stiffness studies.

Discontinuous Flow at 4.2°K. In agreement with Basinski's findings,¹⁶ discontinuous flow in the fine-grained wrought material at 4.2°K was somewhat rare. A slightly more frequent occurrence was noted, however, for the coarse-grained "purified" samples, which fractured after little or no necking (Table I). That discontinuous flow was associated with localized slip was shown by the slip-band clusters often observed on the surface of single crystals after such flow, Fig. 9.

Most single crystals oriented near [111] underwent discontinuous flow, as shown in Fig. 10, in general agreement with the data of Hosford, Fleischer, and Backofen,²⁵ who tested aluminum single crystals of [111], [100], [112], and [123] orientations at 4.2°K and found discontinuous flow only in the [111] crystal. Criteria based on true tensile stress, resolved shear stress, and so forth, were sought to explain the orientation dependence of discontinuous flow, Fig. 10, but none gave consistent results. Such an

orientation dependence is probably related to the nucleating process as discussed by Basinski,¹⁶ who has pointed out that some prior concentration of slip (the nucleating deformation) must take place before the thermal softening can overcome the strain and strain-rate hardening.

Fracture Transition. The transition at 40° to 45°K for the fine-grained wrought samples, Table I, may be reasonably explained by the adiabatic shear argument, which relies chiefly on the rapid decrease in the volume specific heat at low temperatures.

The shear fracture of single crystals at 4.2°K occurred by localized glide along closely parallel slip planes, Fig. 11, similar to that observed in an Al-2 wt pct Mg single crystal by Basinski.¹⁶ No evidence for cracking could be found from examination of partially sheared samples such as that illustrated in Fig. 11. At the same time, the narrow shear band through the polycrystal of Fig. 12 emphasizes again the similarity of fracturing in single crystals and polycrystals.

Effect of Machine Stiffness. In a “purified” sample tested at 4.2°K with the extra-hard arrangement, Fig. 1, suppression of shear fracture was noted. Instead of planar shear after little or no necking, as observed with the standard hard machine, the necking was severe and the fracture surface consisted of a series of small shear steps, so that macroscopically it was oriented nearly at right angles to the tensile axis.

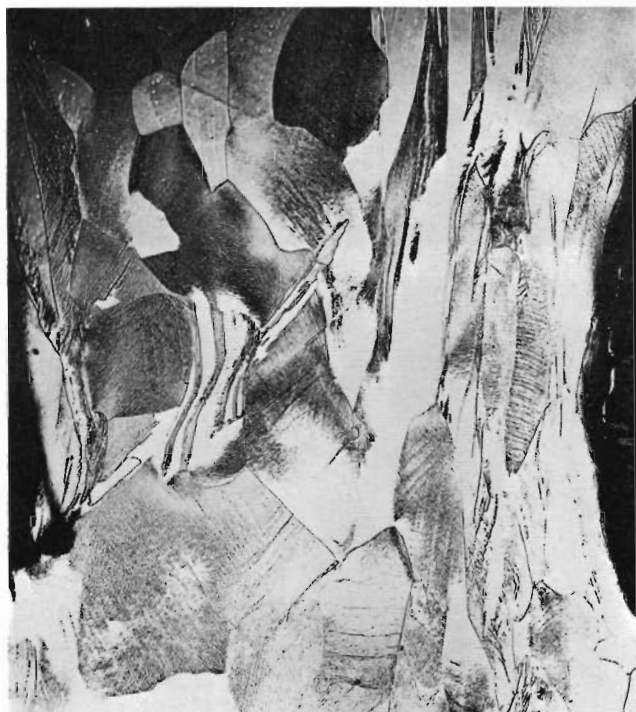


Fig. 12—Arrested shear fracture of a “purified” sample tested in tension at 4.2°K. Some regions within the shear band have recrystallized after testing. Sample was sectioned along the tensile axis, electropolished, and etched with 5 pct HF. X50. Reduced approximately 3 pct for reproduction.

With the soft arrangement, the “purified” and the zone-refined samples failed by shear as with the standard hard machine, Table I. Since the latter was already soft enough to allow shear fracture, a softer system was really not expected to have any effect on the type of fracture. However, if a sample were to undergo frequent discontinuous slip, the shear fracture would be expected to occur after smaller extensions in the softer system. Such reasoning explains the fact that a [111] single crystal fractured in the soft machine at a resolved shear stress of only $\tau_{sf} = 15,400$ psi, considerably lower than the average value of 22,000 psi from the hard-machine tests.

When fine-grained wrought specimens were tested at 4.2°K in the soft machine, an unexpected change in the fracture mode was encountered. Although this material had failed by shear after 65 pct necking in the standard hard machine, the fracture now was of the double-cup type. The most probable reason is a temperature rise in the necked region. It is possible that the rapid flow allowed by the soft system acted to raise the temperature of the neck above the transition level of 40° to 45°K before adiabatic shear could occur. Assuming conversion into heat of the deformation energy from start of necking to fracture, the average temperature rise in the neck may be calculated to be 140°K.

The Rupturing Process. The rupturing process in the single crystals tested at 77°K and above, Table I, proceeded mainly by the operation of two slip systems of primary and conjugate relationship that resulted in a progressive thinning of the neck. Rupture in the polycrystalline “purified” and zone-refined materials followed a broadly similar pattern. Contrary to the observations of Rosi and Abrahams¹³ on silver, copper, and Cu-0.1 at. pct Al single crystals and of Koppenaal³¹ on Cu-10 at. pct Al single crystals, no voids were detected in the aluminum samples after rupture. And since there

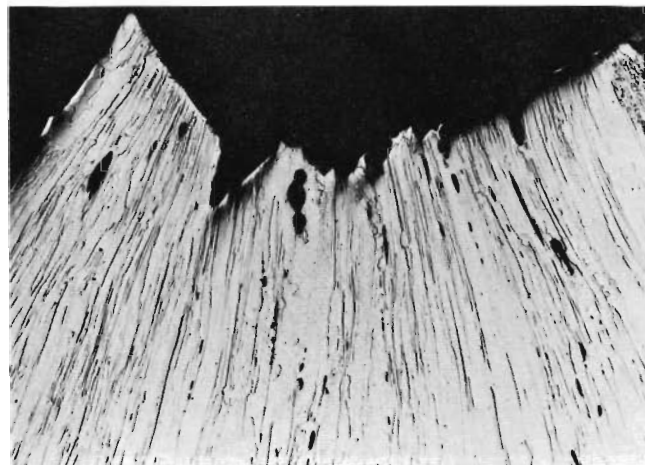


Fig. 13—Appearance of voids in double-cup fracture of a fine-grained wrought sample tested at 45°K with the standard hard machine. Sample was sectioned along the tensile axis, electropolished, and etched with 5 pct HF. X150. Reduced approximately 25 pct for reproduction.

was continual thinning to 100 pct necking, dislocation pile-up cracking as envisaged by Beavers and Honeycombe¹⁹ was a highly unlikely possibility.

The Double-Cup Fracture. In agreement with previous findings^{2,3} the double-cup fracture in fine-grained wrought samples tested above the transition temperature with the standard hard machine, Table I, started with growth and coalescence of voids formed around inclusions. Void formation at smaller strains was seen to be responsible for the decrease of percent necking-at-fracture (pct N) upon lowering temperature, Fig. 5; while many voids were observed below 77°K, Fig. 13, none were detected in a specimen unloaded after as much as 95 pct necking at 295°K. Below the transition temperature, adiabatic shear contributed further to reduce the necking-at-fracture.

Observations of Low-Temperature Grain Boundary Cracking. Besides the appearance of voids, a small number of grain boundary cracks (about one in fifty grains) were observed in all materials tested at very low temperatures. Several examples of such cracks are given in Fig. 14. Briefly, the findings were:

1) In wrought material, grain boundary cracks were detected only at 40°K and below, the number increasing somewhat with lower temperature.

2) Grain boundary cracking was observed even in the zone-refined material; hence the process cannot be ascribed to a brittle film at the boundary.

3) There was a tendency for the grain boundary cracks to lie in a direction at about 45 deg to the specimen axis. This is illustrated in the histogram of Fig. 15, obtained from seven sectioned and polished specimens fractured at 4.2°K.

Metallographic observations of a large number of grain boundary cracks indicated a preference for triple points and an association with deformation "folding",³² Fig. 14. Such features, in addition to the cracking tendency along 45-deg boundaries, suggested boundary shearing, a notion later verified by surface metallography, Fig. 16. While grain boundary shear in aluminum has been observed at temperatures as low as 295°K,³³ boundary cracking has been detected only under fatigue conditions.³⁴ In other materials, Hauser *et al.*³⁵ have noted grain boundary shearing and cracking in magnesium at

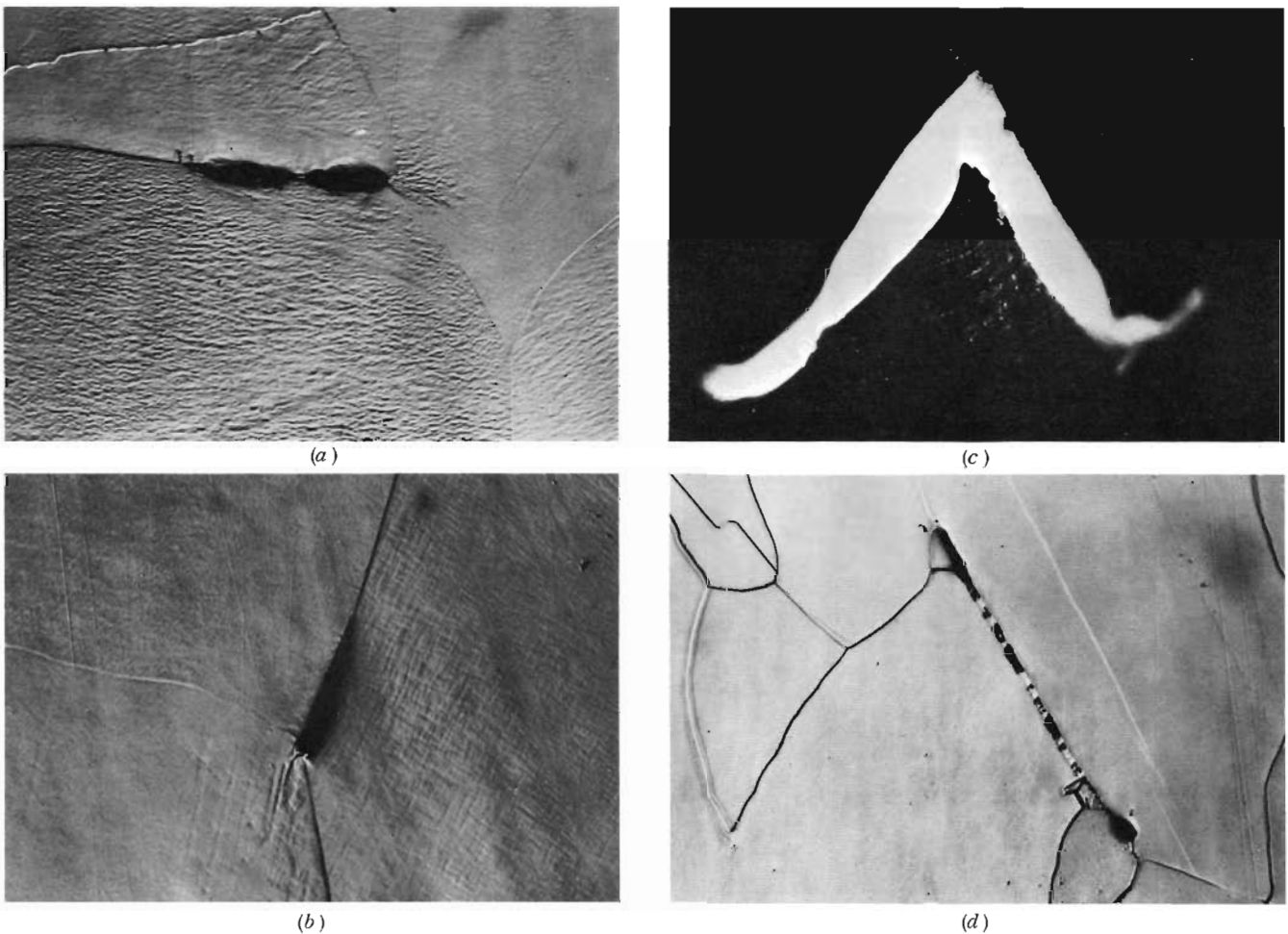


Fig. 14—Examples of grain boundary cracking. Material: (a), (b), (c)—“purified” material; (d)—zone-refined material. Preparation: (a), (b), (d)—sectioned along tensile axis, electropolished, and etched with 5 pct HF; (c)—as deformed surface, photographed in polarized light. Magnification: (a) X250, (b) X500, (c) X50, (d) X250. Note “folding” at triple point in (a) and (b). Structure in (d) has recrystallized after fracture. All samples tested at 4.2°K.

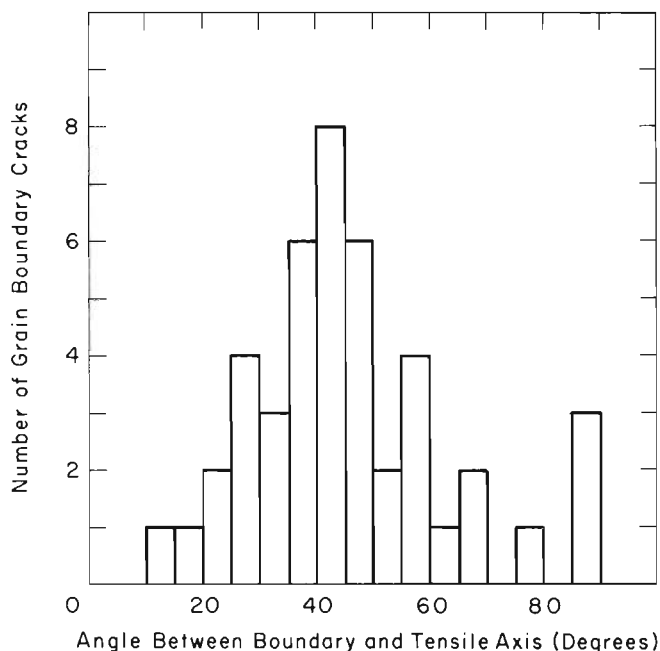


Fig. 15—Histogram of grain boundary cracking. Data obtained from random sectioning (near the center) of seven samples fractured at 4.2°K.

77°K, while boundary shear in iron at 4.2°K has been reported by Gindin and Starodubov.³⁶

DISCUSSION

Fracture by Void Formation. In the inclusion-populated wrought material, the necking-at-fracture decreased rapidly below 77°K (Table I, Fig. 5) because of void formation at smaller and smaller strains. The explanation is that, as temperature is lowered, the strength of the inclusion-matrix interface (or of the inclusion) does not increase as much as the flow stress of the matrix. Therefore less strain is required, with a falling temperature, before interface separation begins.

Several studies support the concept of interface strength as governing void nucleation in ductile fracture. Hertzberg and Kraft³⁷ have reported that in a Cr-Cu alloy the strong interface between chromium whiskers and the copper matrix remained intact at fracture. While studying the pore mechanism of ductile fracture by embedding polystyrene balls as inclusions in plasticine, Rhines³⁸ noted that the reduction-of-area could be increased substantially if the specimens were aged so as to obtain a better wetting between polystyrene and plasticine. Wetting between aluminum and its oxide is considered good,³⁹ which may account for the difficulty of void formation here. Likewise, the ease of void formation in copper as observed by Puttick³ and Rogers⁴ may be explained by the weak cohesion between copper and its oxide inclusions.

Backofen and Hundy¹¹ found that a torsional prestrain greater than one at the surface of round specimens of several materials was sufficient to decrease the subsequent tensile fracture stress and

Fig. 16—Grain boundary sliding indicated by displaced tool markings and scratches. "Purified" sample tested at 4.2°K. X1000. Reduced approximately 21 pct for reproduction.



strain markedly. The fracturing behavior of commercial-purity aluminum, however, was not altered by torsional prestrain up to a value of 6; high-purity aluminum followed the same trend, a mild alteration in properties being observed only after a prestrain greater than 4. A strong cohesion at the inclusion matrix in aluminum may well account for the apparent anomaly with respect to this material.

It is to be noted that the double-cup fracture in aluminum is merely one form of separation in inclusion-populated materials that seems to occur at a relatively high-purity level, the usual fracture in commercial products such as tough-pitch copper and alloyed aluminum being cup-and-cone. The dependence on purity may be rationalized with Fig. 17. Fig. 17(a) represents the necked section of a specimen where void coalescence has produced a lens-shaped crack. Subsequent growth can take place either by general deformation, Fig. 17(b), or localized shear, Fig. 17(c). The latter would be favored by reduced strain hardening and plane-strain deformation,^{14,17} so that it ought to occur at some late stage of growth. In the relatively pure material, growth may be expected to continue by this process, Fig. 17(c), each growth step shifting the crack tip so as to initiate a new shear band in the way shown by broken lines; the end result will be double-cup fracture. As demonstrated by the soft-machine tests at 4.2°K on the fine-grained wrought samples, any heat generated by fast straining is apparently insufficient in itself to induce cone formation in high-purity material. In a sufficiently impure material, however, the situation must be different. As growth occurs by localized shear, new voids may be generated within the band^{4,5} together with a realignment of voids already formed into the plane of the band,^{10,17} Fig. 17(d), so that the effective band area is reduced; relatively lower particle-matrix cohesion as well as adiabatic softening would contribute further to this development. Instead of continued growth by the deformation being shifted to a new band, as in double-cup fracture, strain would be confined to the weakened band by the increased shear stress acting upon it. The final fracture could then be a combination of shearing

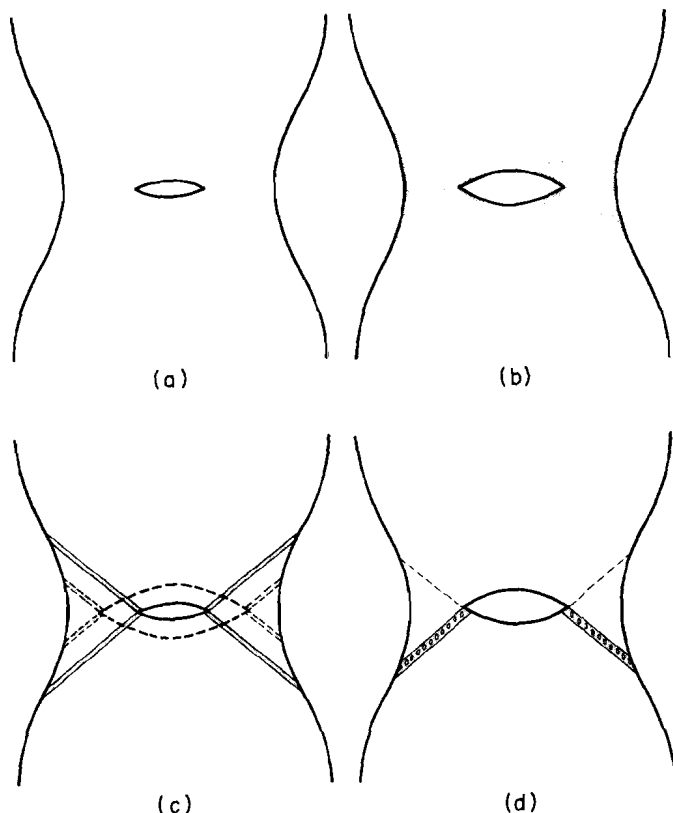


Fig. 17—Crack growth in tensile fracture. (a) Initial crack formation by void coalescence. (b) Crack growth by general deformation within shaded region. (c) Alternative mode of growth by localized shear; double-cup fracture results from continuation of this process as indicated by the broken-line configuration. (d) Void nucleation and realignment weakening the shear band and confining deformation there, with cup-and-cone fracture as a final result.

and tensile separation along the conical surface (the weakened band) as suggested by Cottrell.⁷

In OFHC copper studied by Rogers,⁴ early crack growth seems to occur by a “void-sheet” mechanism due to shear-strain concentration ahead of the crack tip, rather than by general deformation, Fig. 17(c). Presumably, the former process is favored by a high flaw density and ease of void nucleation.

Adiabatic Shear. This has been encountered in a variety of deformation modes. It has even been recognized in an area as superficially removed from metal fracture as seismic faulting.⁴⁰ Yet there has been surprisingly little attempt to interrelate the variables responsible for the basic plastic instability.¹² One may start with the present case of low-temperature discontinuous tensile flow, in which instability arises if an increment of elongation produces locally a thermal softening larger than the strain and strain-rate hardening. Neglecting the lesser strain-rate effect, this condition is given as

$$-\left(\frac{\partial \sigma}{\partial T}\right)_{\epsilon} \frac{dT}{d\epsilon} \geq \left(\frac{\partial \sigma}{\partial \epsilon}\right)_T \quad \text{or} \quad \sigma^{*2} \geq \frac{c_p}{-\alpha \frac{1}{\sigma} \left(\frac{\partial \sigma}{\partial T}\right)_{\epsilon}} \left(\frac{\partial \sigma}{\partial \epsilon}\right)_T \quad [1]$$

where σ^* is the minimum stress to initiate discontinuous flow; $(\partial \sigma / \partial \epsilon)_T$ is the slope of the isothermal stress-strain curve; $(1/\sigma)(\partial \sigma / \partial T)_{\epsilon}$ is the fractional change of flow stress with temperature; and $\alpha \leq 1$ depending upon how nearly adiabatic the deformation. For aluminum at 4.2°K, $c_p = 0.12$ psi per °K,⁴¹ and $(1/\sigma)(\partial \sigma / \partial T)_{\epsilon} = -0.0025^{\circ}\text{K}^{-1}$.⁴² Assuming $\alpha = 1$, [1] becomes $\sigma^{*2} \geq 50(\partial \sigma / \partial \epsilon)_T$. The maximum value of $(\partial \sigma / \partial \epsilon)_T$ is found at yielding and for aluminum at 4.2°K is somewhat less than 10^6 psi. Taking $(\partial \sigma / \partial \epsilon)_T$ as 10^6 , $\sigma^* \geq 7000$ psi, a value slightly higher than the yield stress.* Thus, if deformation

Implicit in this argument leading to $\sigma^ \geq 7000$ psi is an assumption that the system is perfectly soft, or that K , the “spring constant,” is zero. The argument is shortened by the assumption, and the conclusion is not basically different from that reached by recognizing that K is much greater than zero.

were adiabatic ($\alpha = 1$), discontinuous flow ought to start soon after yielding. That it did not is most probably a result of the initial value of α being too low.

From heat-flow considerations, α can be shown to depend on the ratio $l/\sqrt{\kappa t}$, where l is the thickness of the flowing zone, κ the thermal diffusivity, and t the time of flow. In high-purity aluminum at low temperature, κ is high; hence a relatively large l is required to increase α and so establish the inequality of [1]. To this end, an appreciable amount of prior deformation (the nucleating deformation)¹⁶ has to be concentrated in a sufficiently thick zone within a very short time. It is this nucleating deformation that must somehow be related to the orientation dependence of discontinuous flow in the single crystals, Fig. 10. Ordinarily in high-purity aluminum tested at 4.2°K, the energy for nucleating a load drop may be supplied by lightly tapping the machine.

In the 2024 aluminum alloy, κ and therefore the required l are much smaller than in pure aluminum; hence the energy liberated in forming regular slip bands may be sufficient to nucleate discontinuous flow from the beginning.¹⁶ On this basis, nucleation ought to be extremely easy in polymeric materials, with values of κ several orders of magnitude smaller than those for pure metals.

In iron, the nucleating deformation can be supplied in the initial yield drop; thus, in some iron samples tested at low temperatures, a local adiabatic condition is established right at yielding, often leading to fracture under continuously decreasing load.^{43,44}

The implication of adiabatic shear may be extended to other than problems of testing. In deformation processing operations such as rolling or extrusion, the temperature rise in a plastic-elastic transition zone is increased by higher processing speed (contributing to more nearly adiabatic straining) and by a narrowing of the zone (acting to increase local shear-strain rate). The latter would be aided by an approach towards nonhardening or “perfect” plasticity. Thus shear cracks may have

their origins in an adiabatic flow with a flaw re-alignment in such zones.

In a creep-instability theory of seismic faulting, Rowan⁴⁰ has proposed that the earth's mantle at great depths is crystalline and, being hot, can undergo quasi-viscous creep. Since the creep process produces structural defects such as voids and grain boundary cracks, deformation will tend to become confined to narrow zones of shear in which the defects have reduced the effective stress-carrying cross section. The localized deformation then becomes self-accelerating as the structural defects within the zones increase and as the local temperature rises, finally leading to local melting and faulting. Adiabatic shear from this source can also be considered with reference to an inequality similar to [1]. Since stress in creep is more dependent on strain rate ($\dot{\epsilon}$) than on strain, [1] may be modified as

$$\sigma^{*2} \geq \frac{c_p}{-\alpha \frac{1}{\sigma} \left(\frac{\partial \sigma}{\partial T} \right)_{\dot{\epsilon}}} \left(\frac{\partial \sigma}{\partial \dot{\epsilon}} \right)_T \frac{d\dot{\epsilon}}{d\epsilon} \quad [2]$$

The main point about [2] is that at very high strain rates α approaches unity (adiabatic conditions) while $(\partial \sigma / \partial \dot{\epsilon})_T$ diminishes to negligible values, so that the inequality becomes more and more favorable.

The fulfillment of [1] or [2], it is noted, means only that conditions are *favorable* for adiabatic shear. The *duration* of an unstable flow, on the other hand, depends highly on the elastic energy stored in the deforming system and can be shown to be roughly proportional to $\sqrt{m/k}$, where m and k are the effective mass and stiffness of the elastic members. For this reason, the low-temperature discontinuous flow and resulting shear fracture were suppressed by the extra-hard arrangement in the present study. Relative to processing systems, tool designs acting to increase stiffness could be of value in controlling and suppressing the various examples of shear cracking. The role of effective mass, however, is more complex. Although a massive loading system would extend the duration of unstable flow, its high inertia should have the desirable effect of making initiation more difficult.

Grain Boundary Shearing and Cracking at Low Temperatures. For obvious reasons, the grain boundary shear observed at low temperatures cannot be regarded as a sliding between viscous layers. Instead, it is proposed that such sliding occurs when the flow stress exceeds the inherent grain boundary shear strength.

The argument may be summarized in a modified "equicohesive-temperature" diagram. Three solid curves are shown in Fig. 18; besides the two familiar curves representing the flow stress of the crystal and the viscous boundary strength, a third curve, for the inherent boundary strength, is introduced. In current thinking, the grain boundary is regarded as a transition lattice two or three atom layers thick.

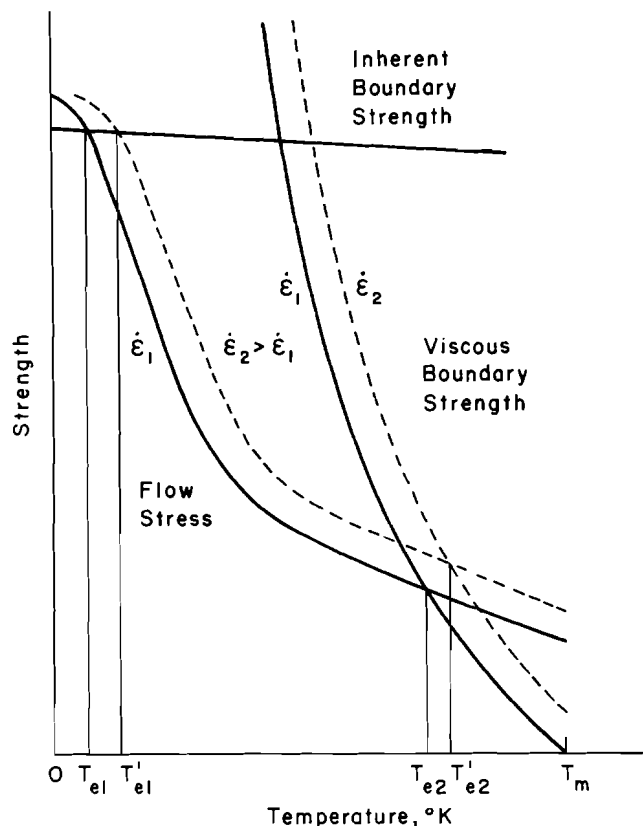


Fig. 18—Modified "equicohesive-temperature" diagram. Broken curves refer to higher strain rate, $\dot{\epsilon}$. T_m , melting point; T_{e1} , T'_{e1} , T_{e2} , T'_{e2} , all equicohesive temperatures.

Except for some atomic disregistry, the boundary resembles a crystal plane, and, as such, has an inherent shear strength. This value would be somewhat less than that for a perfect crystal and depend on temperature only through the elastic modulus, accounting for the rather flat curve in Fig. 18. The steep rise in the flow stress at low temperatures is the result of increased strain hardening, while the viscous boundary strength varies according to the temperature effect on viscosity. The two broken curves in Fig. 18 are for higher strain rate; there is no effect of strain rate on the inherent boundary strength.

Two equicohesive temperatures are noted in Fig. 18. Grain boundary shear above the well-known T_{e2} is generally achieved by *lowering* the viscous boundary strength (enforcing a low creep rate) to a level under the flow stress; sliding below T_{e1} , on the other hand, results from *raising* the flow stress by strain hardening to the level of the inherent boundary strength of about $G/30$, or roughly 130,000 psi for aluminum, Fig. 19. The maximum (macroscopic) shear stress attained in the present tests below 40°K was 40,000 to 70,000 psi, a factor of only 2 to 3 below the theoretical estimate which might easily have been reached in regions of stress concentration such as triple points at the ends of the 45 deg boundaries.

One implication in this view of boundary sliding

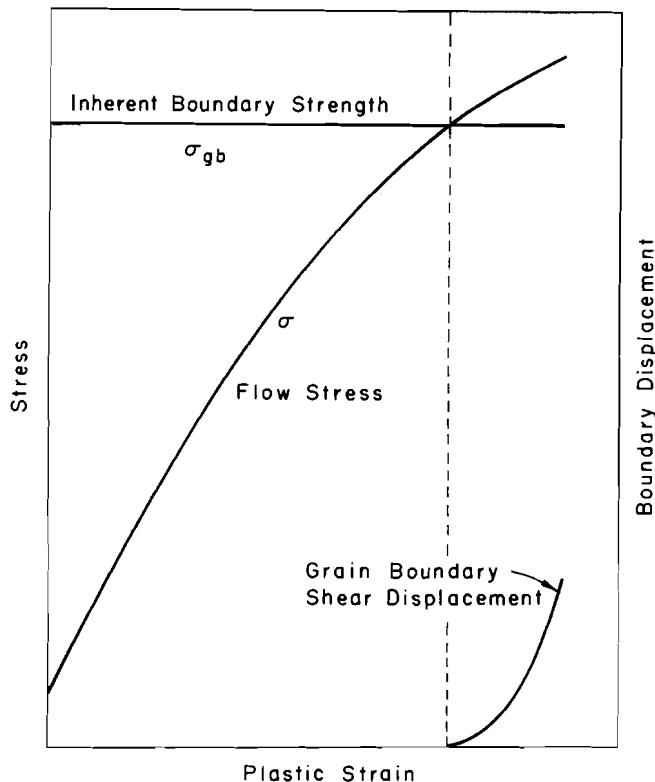


Fig. 19—Tensile test below T_{e1} . Grain boundary sliding starts when $\sigma > \sigma_{gb}$.

bears on the effect of strain rate (broken curves in Fig. 18). While boundary shearing at the high-temperature end of Fig. 18 is suppressed by an increased rate, the opposite is true at low temperatures. To determine whether T_{e1} could in fact be raised above 40°K in this way, two Charpy specimens of polycrystalline aluminum (99.995 pct pure) were fractured by impact, one at 77°K and the other at 295°K. Metallographic examination after sectioning and polishing did indeed reveal grain boundary cracks in the 77°K specimen, although none were detected in the 295°K sample.

Since grain boundary shear has been established at temperatures as low as 4.2°K, this process cannot simply be ruled out in any situation by temperature arguments alone. Rather, the decision must be made as to whether the level of boundary strength (itself a complex quantity) has been reached under the conditions of deformation.

SUMMARY AND CONCLUSIONS

Several conclusions may be drawn from the present work. Although they are based on experiments with aluminum, it is reasonable to expect that they apply generally to ductile metals.

1) The tensile deformation of "inclusion-free" materials at normal temperatures (around room temperature) ends in rupture (~100 pct RA); at very low temperatures (around 4.2°K), fracture is still purely plastic but now brought on by adiabatic shear. In these experiments there was no evidence

of void nucleation by vacancy condensation, nor was any support found for dislocation pile-up cracking.

Fracture of inclusion-populated materials over a range of temperatures is nucleated with the formation of voids as the local tensile stress exceeds the strength of the inclusion-matrix interface or of the inclusion itself. Crack growth begins with void coalescence, and in the early stage proceeds by general deformation in the neck; at a later stage, growth may involve localized shear. Final separation can occur in either one of two ways: if the material is relatively pure (free of inclusions), continued growth by localized shear results in the double-cup fracture; if impure, creation of voids and realignment of existing voids along the shear bands confine deformation there and lead to a cup-and-cone fracture.

2) Adiabatic shear in low-temperature discontinuous flow requires a transient energy pulse, such as that provided by tapping the machine or obtained from a local concentration of slip. Other sources of local temperature rise for an unstable flow (and fracture) may be imagined, however, as in the various deformation processing operations or in the deformation responsible for seismic faulting.⁴⁰ Once initiated, the duration of unstable flow is controlled by the effective mass and elastic stiffness of the deformation system.

3) Grain boundary cracking in aluminum at 40°K and below was established to be a result of grain boundary shear, showing that viscous flow is not necessary for boundary sliding. Instead, a low-temperature boundary shear may occur when the local stress in regions such as triple points is elevated to the level of the inherent boundary shear strength.

ACKNOWLEDGMENTS

The authors wish to thank the U.S. Atomic Energy Commission for the support of this work under Contract No. AT(30-1)-1310. One of the authors (G. Y. Chin) was the recipient of a Cooperative Fellowship from the National Science Foundation. The Aluminum Company of America generously supplied the aluminum. The effort of Dr. L. M. Foster of the Alcoa Research Laboratory in providing the zone-refined material is gratefully acknowledged. Many helpful discussions were held with Dr. M. L. Ebner.

REFERENCES

- ¹P. Ludwik: *Z. Metallk.*, 1926, vol. 18, p. 22.
- ²C. F. Tipper: *Metallurgia*, 1948-49, vol. 39, p. 133.
- ³K. E. Puttick: *Phil. Mag.*, 1959, vol. 4, p. 964.
- ⁴H. C. Rogers: *Trans. Met. Soc. AIME*, 1960, vol. 218, p. 498.
- ⁵C. Crussard, J. Plateau, R. Tambaker, G. Henry, and D. Lajunesse: *Fracture*, p. 524, John Wiley and Sons, New York, 1959.
- ⁶B. Y. Pines: *Zh. Eksperim. i Teor. Fiz.*, 1946, vol. 16, p. 744.
- ⁷A. H. Cottrell: *Fracture*, p. 20, John Wiley and Sons, New York, 1959.
- ⁸H. H. Bleakney: *Can. Metals*, February, 1957, vol. 20, p. 60.
- ⁹P. W. Bridgman: *Fracturing of Metals*, p. 246, ASM, Cleveland, Ohio, 1948.

- ¹⁰W. A. Backofen, A. J. Shaler, and B. B. Hundy: *Trans. Am. Soc. Metals*, 1954, vol. 46, p. 655.
- ¹¹W. A. Backofen and B. B. Hundy: *J. Inst. Metals*, 1953, vol. 81, p. 433.
- ¹²W. A. Backofen: ASM Conference on Fracture of Engineering Materials, Rensselaer Polytechnic Institute, Troy, N. Y., August, 1959, to be published.
- ¹³F. D. Rosi and M. S. Abrahams: *Acta Met.*, 1960, vol. 8, p. 807.
- ¹⁴C. Zener: *Fracturing of Metals*, p. 3, ASM, Cleveland, Ohio, 1948.
- ¹⁵P. Winchell: Sc. D. thesis, M.I.T., 1958.
- ¹⁶Z. S. Basinski: *Proc. Roy. Soc. (London), Ser. A*, 1957, vol. 240, p. 229.
- ¹⁷K. E. Puttick: *Phil. Mag.*, 1960, vol. 5, p. 759.
- ¹⁸P. B. Hirsch: *Internal Stresses and Fatigue in Metals*, p. 139, Elsevier Publishing Co., Amsterdam and New York, 1959.
- ¹⁹C. J. Beevers and R. W. K. Honeycombe: *Phil. Mag.*, 1962, vol. 7, p. 763.
- ²⁰J. E. Neimark: Sc. D. thesis, M.I.T., 1959.
- ²¹G. Y. Chin and W. A. Backofen: *J. Inst. Metals*, 1961-62, vol. 90, p. 13.
- ²²J. Holden: *Phil. Mag.*, 1961, vol. 6, p. 547.
- ²³D. H. Avery and W. A. Backofen: in *Fracture of Solids*, p. 339, Interscience Publishers, New York, 1963.
- ²⁴C. M. Glass, G. L. Moss, and S. K. Golaski: *Response of Metals to High Velocity Deformation*, p. 115, Interscience Publishers, New York, 1961.
- ²⁵W. F. Hosford, Jr., R. L. Fleischer, and W. A. Backofen: *Acta Met.*, 1960, vol. 8, p. 187.
- ²⁶R. P. Carreker, Jr. and W. R. Hibbard, Jr.: *AIME Trans.*, 1957, vol. 209, p. 1157.
- ²⁷C. J. Beevers and R. W. K. Honeycombe: *Fracture*, p. 474, John Wiley and Sons, New York, 1959.
- ²⁸R. Armstrong, I. Codd, R. M. Douthwaite, and N. J. Petch: *Phil. Mag.*, 1962, vol. 7, p. 45.
- ²⁹R. W. Armstrong: *J. Mech. Phys. Solids*, 1961, vol. 9, p. 196.
- ³⁰G. I. Taylor: *J. Inst. Metals*, 1938, vol. 62, p. 307.
- ³¹J. J. Koppenaal: *Acta Met.*, 1961, vol. 9, p. 1078.
- ³²H. C. Chang and N. J. Grant: *AIME Trans.*, 1956, vol. 206, p. 544.
- ³³F. B. Cuff, Jr. and N. J. Grant: *Trans. Met. Soc. AIME*, 1958, vol. 212, p. 355.
- ³⁴G. C. Smith: *Proc. Roy. Soc. (London), Ser. A*, 1957, vol. 242, p. 189.
- ³⁵F. E. Hauser, P. R. Landon, and J. E. Dom: *Trans. Am. Soc. Metals*, 1956, vol. 48, p. 986.
- ³⁶I. A. Gindin and Ya. D. Starodubov: *Soviet Phys.-Solid State*, 1959, vol. 1, p. 1642.
- ³⁷R. Hertzberg and R. W. Kraft: *Trans. Met. Soc. AIME*, 1963, vol. 227, p. 580.
- ³⁸W. J. Rhines: S. M. thesis, M.I.T., 1961.
- ³⁹D. T. Livey and P. Murray: *Warmfeste und Korrosionsbeständige Sinterwerkstoffe*, p. 375, Springer, Berlin, 1956.
- ⁴⁰E. Orowan: *Rock Deformation*, p. 323, Geological Society of America Memoir 79, 1960.
- ⁴¹J. A. Kok and W. H. Keesom: *Physica*, 1937, vol. 4, p. 835.
- ⁴²Z. S. Basinski: *Phil. Mag.*, 1959, vol. 4, p. 393.
- ⁴³H. G. Baron: *J. Iron Steel Inst.*, 1956, vol. 182, p. 354.
- ⁴⁴N. P. Allen, B. E. Hopkins, and J. E. McLennan: *Proc. Roy. Soc. (London), Ser. A*, 1956, vol. 234, p. 221.

The Surface Diffusion of Germanium on Copper

P. G. Shewmon and J. Y. Choi

The surface-diffusion coefficient for Ge^{68} , $D_s(Ge)$, has been measured on (111) and (100) surfaces of copper from 1000° to 620°C. $D_s(Ge)$ on the (111) is two to three times that on the (100) as was found earlier for copper and gold on copper. $D_s(Ge)$ on both (111) and (100) is about thirty times that found for gold or copper tracers on the same surfaces, while in the temperature range where both $D_s(Ge)$ and $D_s(Au)$ have been measured the activation energy for germanium is the same as that for gold. The apparent activation energy for $D_s(Ge)$ is not a constant, but decreases with temperature.

IN a recent paper we reported on the application of a new tracer technique to the determination of the surface-diffusion coefficient (D_s) for gold and copper on (111) and (100) surfaces of copper.¹ In this paper, we shall give the results obtained when the

same technique was used to measure D_s for germanium on the (111) and (100) surfaces of copper.

In addition to providing data on D_s for an additional element on copper, the longer half-life of germanium (275 days) meant that D_s could be measured down to a much lower temperature and thus over a much wider temperature range (1000° to 620°C) than was used in our gold-tracer work (1060° to 780°C) or copper mass-transport studies (1060° to 800°C).^{2,3} The apparent activation energy for $D_s(Ge)$ is essentially the same as that found for gold or copper in the same temperature range, though the values of $D_s(Ge)$ are thirty times greater than those found for gold or copper tracers.

The most interesting new result found is that the apparent activation energy for $D_s(Ge)$, and thus D_0 , definitely increases with temperature. Such a trend was much more apparent in Gjostein's⁴ mass-transport work on copper than in our own, though in an earlier paper we mentioned the difficulty of fitting all of our points with one straight line.³ No real explanation of this is given though experiments done on grain boundary groove growth at various ambient pressures demonstrate unequivocally that vapor transport plays no part in the increase in activation energy with temperature.

P. G. SHEWMON and J. Y. CHOI, Members AIME, are Associate Professor of Metallurgical Engineering and Research Metallurgical Engineer, respectively, Metallurgy Department, Carnegie Institute of Technology, Pittsburgh, Pa. Manuscript submitted July 15, 1963. IMD